NA62

M. Moulson (resp.),
A. Antonelli, V.Kozhuharov (associato), G. Lanfranchi,
S. Martellotti, M. Martini (associato), M. Soldani (assegnista),
J. Swallow (borsista straniero), G. Tinti, T. Spadaro

in collaboration with
A. Russo, D. Pierluigi, E. Paoletti, R. Tesauro
(Reparto Sviluppo e Costruzione Rivelatori)

The NA62 Experiment

The branching ratios (BRs) for the extremely rare decays $K \rightarrow \pi\nu\overline{\nu}$ are among the observables in the quark-flavor sector most sensitive to new physics. Because these decays are strongly suppressed and their BRs are calculated very precisely in the Standard Model (SM), they are excellent probes for new physics at mass scales of hundreds of TeV, surpassing the sensitivity of B-meson decays in many SM extensions. Observations of lepton-flavor-universality-violating phenomena are mounting in the B sector. Measurements of the $K \rightarrow \pi\nu\overline{\nu}$ BRs are critical to interpreting the data from rare B decays and may demonstrate that these effects are a manifestation of new degrees of freedom, fundamentally disrupting the Standard Model. The SM predicts $BR(K^+ \rightarrow \pi^+\nu\overline{\nu}) = (8.4 \pm 1.0) \times 10^{-11}$. The NA62 experiment at the CERN SPS took data from 2016 to 2018, collecting 20 candidate $K^+ \rightarrow \pi^+\nu\overline{\nu}$ events, allowing this BR to be determined to within about 40%. NA62 resumed data taking in 2021 and should collect about 60 candidate events for a measurement of $BR(K^+ \rightarrow \pi^+\nu\overline{\nu})$ to better than 20% precision by the end of LHC Run 3.

The NA62 experiment [8], illustrated in **Fig. 1**, makes use of a 75 GeV unseparated positive secondary beam. The total beam rate is 750 MHz, providing ~50 MHz of K^+ mesons. The decay volume begins 105 m downstream of the production target. 6 MHz of kaon decays are observed in the 65-m long fiducial vacuum decay region by means of tracking and particle-identification systems. Ring-shaped Large-Angle photon Vetoes (LAVs) are placed at 12 stations along the decay region and provide full coverage for decay photons with 8.5 mrad $< \theta <$ 50 mrad. The last 35 m of the decay region hosts a dipole spectrometer with four straw-tracker stations operated in vacuum. The NA48 liquid-krypton calorimeter (LKr) is used to veto high-energy photons at small angle. Additional detectors further downstream extend the coverage of the photon veto system, including the Small-Angle Calorimeter (SAC), to intercept photons that would exit the experiment through the downstream beam pipe, and the Intermediate Ring Calorimeter (IRC), to provide veto coverage between the LKr and the SAC. The IRC and SAC are collectively referred to as the Small-Angle Vetoes (SAV).
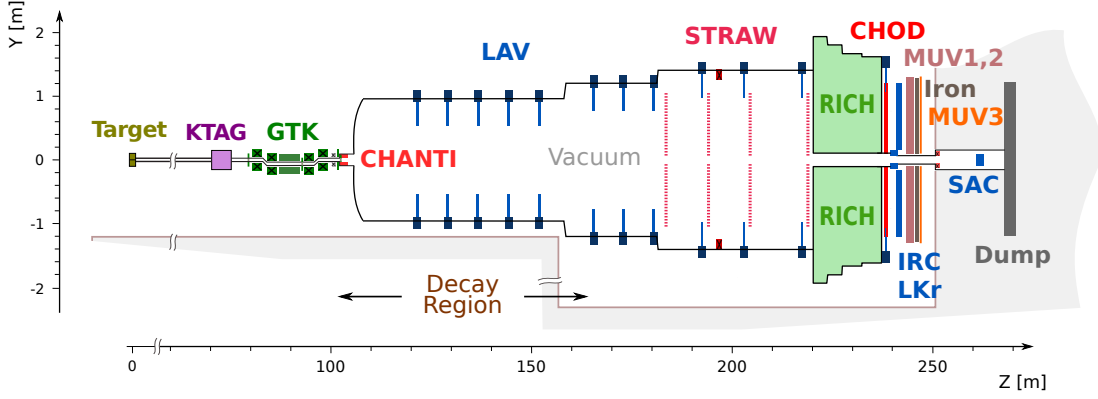
Fig. 1: Schematic view of the NA62 experiment, showing the kaon production target, KTAG Cerenkov K^+ beam tagger, GTK beam tracker, CHANTI collar veto, LAV large-angle photon vetoes, STRAW straw-tube trackers, RICH ring-imaging Cerenkov detector, CHOD hodoscope, MUV1-3 hadron calorimeters and muon vetoes, LKr calorimeter, and IRC and SAC small-angle photon vetoes.

Measurement of the branching ratio for $K^+ \to \pi^+ \nu \bar{\nu}$

The NA62 experiment collected its first data sample in 2016-2018 for a total of about 4×10^{12} kaon decays in fiducial volume. The NA62 in-flight technique for the measurement of BR($K^+ \to \pi^+ \nu \bar{\nu}$) has been established and proven to work. The first physics result on $K^+ \to \pi^+ \nu \bar{\nu}$, based on the 2016 data set, was obtained in 2018 and published in early 2019 [9]; the results of the analyses of the 2017 and 2018 data sets, were published in 2020 and 2021, respectively [10, 11].

The analysis is mostly based on kinematic cuts and particle identification. The invariant $m^2_{miss} = (p_{K+} - p_{\pi+})^2$ is used to discriminate between the signal and background kinematics, where p_{K+} and $p_{\pi+}$ are the K^+ and π^+ 4-momenta, respectively. **Fig. 2** shows the distribution of the selected K^+ decays in the (m^2_{miss}, $P_{\pi+}$) plane, with $P_{\pi+}$ the magnitude of the π^+ 3-momentum. Regions populated mostly by $K^+ \to \pi^+ \pi^0(\gamma)$, $K^+ \to \pi^+ \nu(\gamma)$ and $K^+ \to \pi^+ \pi^+ \pi^-$ are visible. Two signal regions are defined: the region at lower (higher) m^2_{miss} is referred as region 1 (2). The m^2_{miss} resolution is on the order of 10^{-3} GeV^2/c^4 for the $K^+ \to \pi^+ \pi^0(\gamma)$, and this drives the choice of the boundaries of these regions. For the analysis of the 2016 and 2017 data, the momentum range was restricted to $15 < P_{\pi+} < 35$ GeV/c, ensuring at least 40 GeV/c of missing energy, thus significantly improving the efficiency for π^0 detection. For the 2018 data, a broader momentum range was used to define region 2, $15 < P_{\pi+} < 45$ GeV/c, since the $K^+ \to \pi^+ \pi^0(\gamma)$ background was seen to be under control and the $K^+ \to \mu^+ \nu(\gamma)$ background is much lower than in region 1. The momentum cut costs roughly half of the signal acceptance. The calorimeters and RICH provide π^+ identification and the photon veto system ensures rejection of photons with angles from 0 up to 50 mrad with respect to the beam axis.
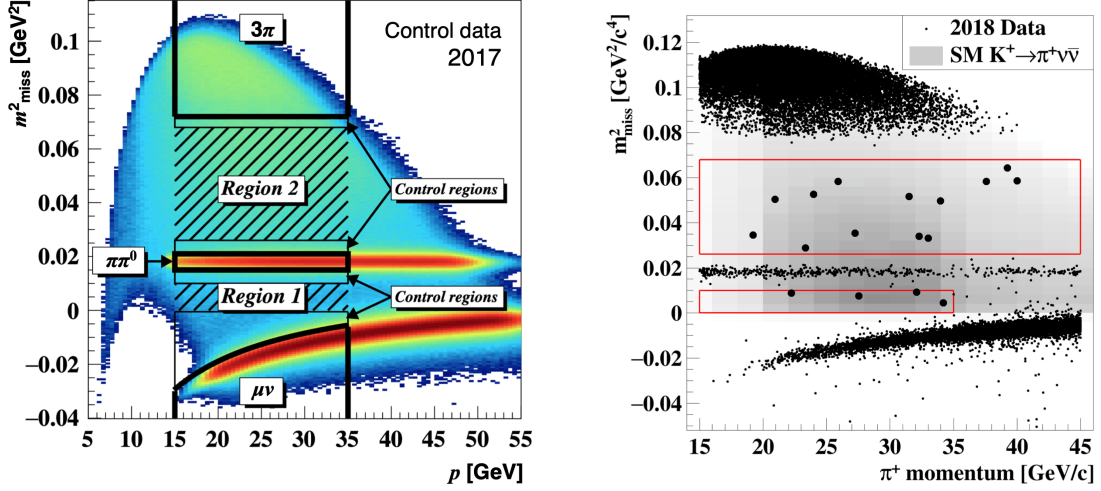
Fig. 2: Left: m^2_{miss} as a function of $P_{\pi+}$ for control data after K^+ decay selection. Signal and background control regions are illustrated, as are regions for the selection of control samples of background events. Right: m^2_{miss} vs. $P_{\pi+}$ distribution for 2018 data, showing 17 selected events.

For the analysis, a blind procedure was adopted, with the signal and control regions kept masked until the evaluation of expected signal and background was completed. Control samples of $K^+ \rightarrow \pi^+\pi^0(\gamma)$, $K^+ \rightarrow \pi^+\nu(\gamma)$ and $K^+ \rightarrow \pi^+\pi^+\pi^-$ decays from data are employed for background studies. The fraction of background events entering each signal region via the reconstructed tails of the corresponding m^2_{miss} peak is modeled with data from these control samples and corrected with MC simulation for biases induced by the selection criteria. An additional source of background is from decays or interactions of K^+ mesons occurring upstream of the final collimator, in which a daughter pion mimics a signal event by being accidentally matched to random beam particles that are nearby in time. The geometrical distribution of these upstream events is used to define the analysis cuts and estimate the background for the selected signal sample.

The measurement of the branching ratio [11] is obtained by combining the data samples from 2016, 2017, and 2018,

$$\mathrm{BR}(K^+ \rightarrow \pi^+\nu\bar{\nu}) = \left(10.6^{+4.0}_{-3.4}\,_{\mathrm{stat}} \pm 0.9_{\mathrm{syst}}\right) \times 10^{-11}$$

from which the $K^+ \rightarrow \pi^+\nu\bar{\nu}$ decay is observed for the first time with 3.4σ significance. This is the most precise measurement so far. It is compatible with the SM expectation to within one standard deviation. The NA62 measurement, together with the preliminary KOTO limit for the analogous K_L branching ratio and theoretical predictions from a number of new-physics models, is illustrated in **Fig. 3**. Some of the models predict large deviations from the SM expectation and seem to be excluded. More precise measurements would help to clarify the situation.
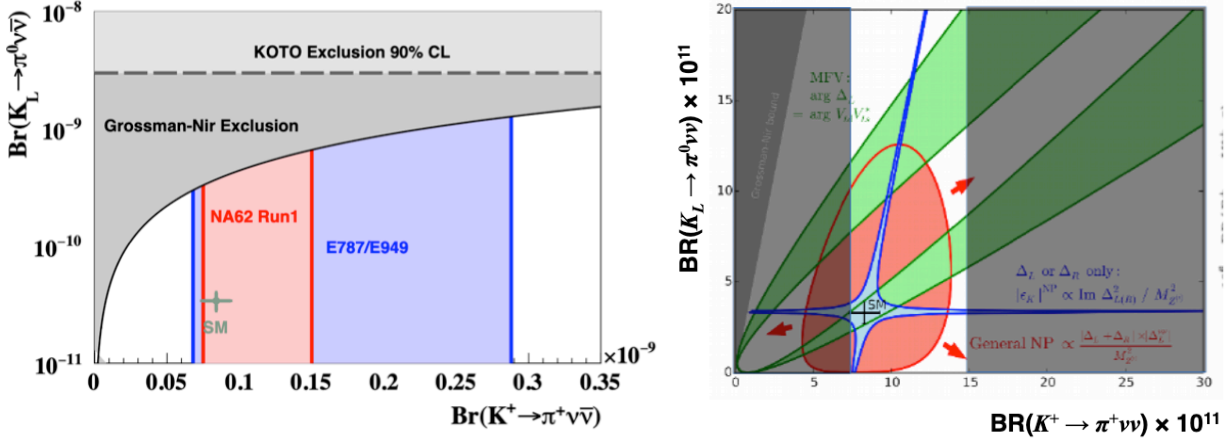
Fig. 3: Comparison between K_L and K^+ branching ratio measurements and different theoretical models. Left: Region allowed by NA62 2016-2018 measurement and model independent Grossman-Nir bound derived from NA62 result. Right: bands of correlation expected from new physics models involving minimal flavor violation (green), new physics deriving from couplings to quarks of definite chirality, e.g., models with modified Z couplings or a Z' coupling to left- or right-handed quarks only (blue), and in new-physics models without these characteristics (red).

NA62 data taking in 2023

During most of 2016-2018 data taking, the beam intensity was kept stable at about 50-70% of the nominal value. This mode of operation was optimized for efficient data taking. Before the restart of data taking in 2021, several modifications were made to the experiment to reduce background from upstream decays and interactions, including the rearrangement of beamline elements around GTK achromat, the addition of a fourth GTK beam tracker station, and the introduction of a new veto hodoscope upstream of the decay volume as well as additional veto counters around the downstream beam pipe. As a result of these modifications, in both 2021 and 2022, the experiment took data at the nominal value of the beam intensity for practically the entire run period. It was then determined that running at 70% of the nominal value optimizes the sensitivity of the experiment, so for 2023, NA62 took data at this intensity. The experiment ran from May to September, for a total of 22 weeks. A short period of data taking was dedicated to running in beam-dump mode as well. With respect to the previous dump-mode running period in 2021, the integrated luminosity expressed in protons dumped on the NA62 collimator, $(2.4\pm0.5)\times10^{17}$ POT, was 70% larger in 2023. The entire beam-dump run was carried out under the guidance and responsibility of the LNF personnel involved.

LNF group responsibilities

The principal responsibility of the NA62 LNF group is in the maintenance, operation, and analysis of data from two of the experiment's main photon detection systems, the

Large-Angle Veto (LAV) system and the Small-Angle Veto (SAV) system, as well as providing general support to the experiment, assisting with run planning and coordination, and participating in data taking and data analysis. In 2023, the group also made significant contributions in the coordination of the exotic physics working group and in feasibility studies for the experimental program after the end of LHC Run 3.

LNF group activities: LAV and SAV systems

In 2023, the LNF group prepared the LAV and SAV systems for the restart of NA62 data taking and operated and monitored the performance of the detectors throughout the 22-week running period. In particular, the group made the following contributions:
- Thorough diagnostics and repair of the LAV and SAV systems in preparation for data taking in 2023.
- Continuous on-call expert support throughout the entire period.
- Improvement and optimization of the simulation and reconstruction code for the LAV and SAV systems.
- Management of data quality, with emphasis on the LAV and SAV detectors.
- Analysis of data acquired in 2021-2023 and measurement of system performance.

The LAV system consists of 12 detector stations arranged at intervals of 6 to 10 m along the vacuum tank along its entire length. Each station consists of four or five rings of lead glass blocks, with the blocks staggered in azimuth in successive rings. The total depth of a five-layer station is 27 radiation lengths. This structure guarantees high efficiency, hermeticity, and uniformity of response. The readout chain for the LAV stations consists of two different types of boards, a dedicated front-end board (LAV-FEE) developed for the LAV detector, and a common digital readout board (TEL62) used by many of the NA62 detectors. The LAV detectors and the front-end electronics were designed and constructed at LNF between 2008 and 2014.

The small-angle veto detectors, SAC and IRC, are shashlyk-type electromagnetic calorimeters that provide veto coverage for photons with polar angles down to zero degrees. They are exposed to a very high rate of photons from kaon decays and, for the IRC, muons from pion and kaon decays. The IRC was assembled at LNF in 2014.

LNF group activities: Analysis of exotic particle decays

Thanks to its high intensity beam and detector performance (redundant particle-identification capability, extremely efficient veto system and high-resolution measurements of momentum, time, and energy), NA62 can achieve sensitivities to long-lived light mediators in a variety of new-physics scenarios. Such feebly-interacting particles are expected to be produced after interaction of the proton beam with the most upstream collimator (TAX), approximately 23 m downstream of the NA62 target T10. The decay of these "exotic" mediators into SM particles are searched

for in the NA62 decay volume, more than 100 m downstream of T10. A dedicated setup has been used for dedicated data-taking periods, in which the T10 target is lifted and the entire proton beam is dumped into the TAX collimator (beam-dump, or BD, mode). The corresponding analyses and activities are a responsibility of the LNF group.

Three analyses have been completed based on a data sample taken in 2021 and corresponding to $(1.40\pm0.28)\times10^{17}$ POT:

- A search for Dark photons or Axion-like particles decaying to $\mu^+\mu^-$ final states, published in JHEP [1];
- A search for Dark photons decaying to e^+e^- final states, submitted to PRL [6];
- A search for Dark photon, Axion-like particle or Dark scalar decays to hadronic final states, presented at Moriond QCD 2024 [21]. The final states probed were the following: $\pi^+\pi^-$, $\pi^+\pi^-\pi^0$, $\pi^+\pi^-\pi^+\pi^-$, K^+K^-, K^+, $\pi^+\pi^-\gamma$, $\pi^+\pi^-\eta$

All above-mentioned analyses profit from a "pointing approach": the total vertex momentum is extrapolated backwards to the point of closest approach to the nominal proton impact point on the TAX. As the signal is produced from proton interactions, it accumulates in a well-defined region in the plane of the distance of closest approach (CDA_{TAX}) vs the longitudinal position of the minimum approach point (Z_{TAX}). Signal and control regions, labelled SR and CR, are defined and kept masked until the analysis blessing.

The background to the above analyses was determined through a mix of strategies, depending on the mechanisms producing it. To determine the halo-induced background, single muon tracks from an independent trigger line were backward-propagated to a plane preceding the decay-volume. This sample was used as an input to the official NA62 GEANT4-based simulation, to compute muon-induced backgrounds and to predict the expected background in the SR/CR from this component. A dedicated simulation was performed to evaluate the expected backgrounds from the interactions of neutrinos produced within the hadronic showers due to the dumped protons. This component proved to be negligible at the present statistics for any of the above analyses.

A background component was identified for the hadronic analysis, which had been irrelevant for the di-lepton searches performed so far. It stems from K^+ mesons that can pass the non-instrumented hole of the ANTI0 detector. The presence of such mesons can be proved using the RICH detector. The K^+s that decay before being identified in the RICH can undergo decays to hadronic final states, constituting a possible background component. **Fig. 4** shows the distribution of a control sample of data events with tracks not associated to ANTI0 in-time hits, mostly because originating in the ANTI0 hole, in the plane of Z_{VTX} vs the invariant mass of a $\pi^+\pi^-(\gamma)$ decay reconstructed in the fiducial volume (FV). Events with $K^+ \rightarrow \pi^+\pi^+\pi^-$ decays with one π^+ not reconstructed populate the FV for invariant masses below the K^+ mass. This K^+-induced background has been simulated using a selected single-track K^+ sample as a

gun for the NA62 Monte Carlo simulation. The expected background for all final states with hadrons is found to be below 0.04 events. In **Fig. 4**, another component is visible, this time peaking around the K_S mass, due to $K_S \to \pi^+\pi^+$ decays. Missing a complete simulation of such component, a 3 sigma region around the K_S invariant mass has been masked for the preliminary analysis release.
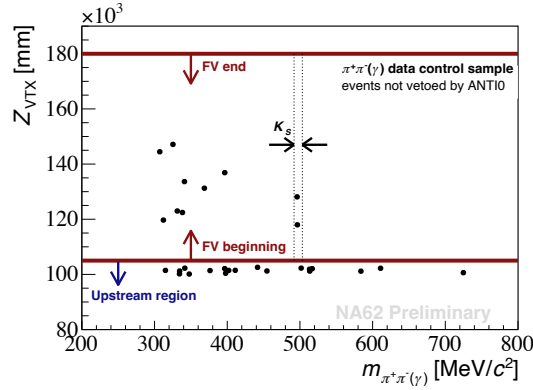

Fig. 4: Events not in ANTI0 acceptance or not vetoed by ANTI0 in Z_{VTX}–invariant mass plane. Solid lines indicate the fiducial volume (FV). Dashed lines indicate the 3-sigma K_S mass window masked for the preliminary result.

Two analyses are in progress on the combined 2021+2023 data-sample:
- A search for axion-like particles decaying to $\gamma\gamma$
- A search for heavy neutral leptons decaying to semi-leptonic channels and open decay channels involving neutrinos.

For the first case, a competitive search result can be expected with the recorded data samples. For the second, we expect to use in the analysis the full envisaged beam-dump statistics of 10^{18} protons dumped on the TAX before LS3.

The LNF group and the future of NA62

Since the start of data taking, the LNF group has had a leading role in planning the future of the rare-kaon decay program at CERN. Before 2020, this effort focused mainly on design studies for KLEVER, an experiment to measure BR($K_L \to \pi^0 \nu \bar{\nu}$) at the CERN SPS with a sensitivity of about 60 signal events at the SM BR and a signal-to-background ratio of about 1 [12]. KLEVER was intended as a follow up on NA62, reusing as much of the existing apparatus as possible, but until recently, the transition path from NA62 to KLEVER was not clearly defined. In particular, possibilities for high-statistics measurements of BR($K^+ \to \pi^+ \nu \bar{\nu}$) decays in a future generation of NA62 were unexplored.

In 2020, a long-term plan for a program at a high-intensity kaon facility was outlined, consisting of the following phases:

1. A high-statistics K^+ experiment to measure BR($K^+ \to \pi^+ \nu \bar{\nu}$) to 5%
2. A transitional experiment making use of a K_L beam for KLEVER and the downstream detector with tracking and PID as in NA62 to investigate other rare K_L decays such as $K_L \to \pi^0 \ell^+ \ell^-$.
3. A high-statistics K_L experiment to measure BR($K_L \to \pi^0 \nu \bar{\nu}$) to 20% (KLEVER)
4. Additional running in beam-dump mode to attain the highest possible precision in searches for exotic physics, as discussed in the previous section, to the maximum extent compatible with the rare kaon decay program.

For the KLEVER phase, extension of the NA62 beamline by 150 m is required to mitigate background from $\Lambda \to n\pi^0$ decays. The K^+ phase therefore seems more likely to be ready by the end of LS4, currently foreseen at the start of 2029. The program outlined above was presented to the CERN SPSC as HIKE—High Intensity Kaon Experiments at the CERN SPS—in a Letter of Intent in November 2022 [13]. The formal proposal for HIKE [14] was submitted in October 2023, with substantial input from the LNF group. At the end of 2023, a final decision on the HIKE program was expected to be announced in March 2024.

For the experimental program outlined above, many of the same detectors would be used in all of the different phases. In particular, the calorimeter and photon veto systems conceptually designed for Phase 3 (KLEVER) would be used starting in Phase 1 (K^+). R&D work on the two important detector systems for future experiments—the main electromagnetic calorimeter, to replace the NA48 LKr calorimeter, and the KLEVER small-angle calorimeter (SAC)—has been in progress at Frascati for the past few years, in part within the framework of the AIDAinnova research infrastructure.

HIKE Main Electromagnetic Calorimeter

It is natural to inquire as to whether the liquid-krypton calorimeter (LKr) [15] currently used in NA62 can be reused for HIKE. Indeed, the efficiency and energy resolution of the LKr appear to be satisfactory for all phases of HIKE. The LKr time resolution, however, is a significant issue. For the K_L phases, and for KLEVER in particular, the calorimeter provides the measurement of the event time, and must have a time resolution of 100 ps or better for the reconstruction of π^0's with energies of a few GeV. Additionally, the size of the LKr inner bore would limit the beam solid angle and hence the kaon flux during the K_L phases.

We are investigating the possibility of replacing the LKr with a shashlyk calorimeter patterned on the PANDA FS calorimeter, in turn based on the calorimeter designed for the KOPIO experiment [16]. This design featured modules 110×110 mm^2 in cross section made of alternating layers of 0.275-mm-thick lead absorber and 1.5-mm-thick injection-molded polystyrene scintillator. This composition has a radiation length of 3.80 cm and a sampling fraction of 39%. The scintillator layers were optically divided into four 55×55 mm^2 segments; the scintillation light was collected by WLS fibres traversing the stack longitudinally and read out at the back by avalanche photodiodes

(APDs). KOPIO was able to obtain an energy and time resolution of 3.3% and 73 ps at 1 GeV with this design, establishing that it is capable of providing the same energy resolution as the LKr while meeting the time resolution requirements for HIKE. For HIKE, the design would be updated to use silicon photomultipliers (SiPMs) instead of APDs.
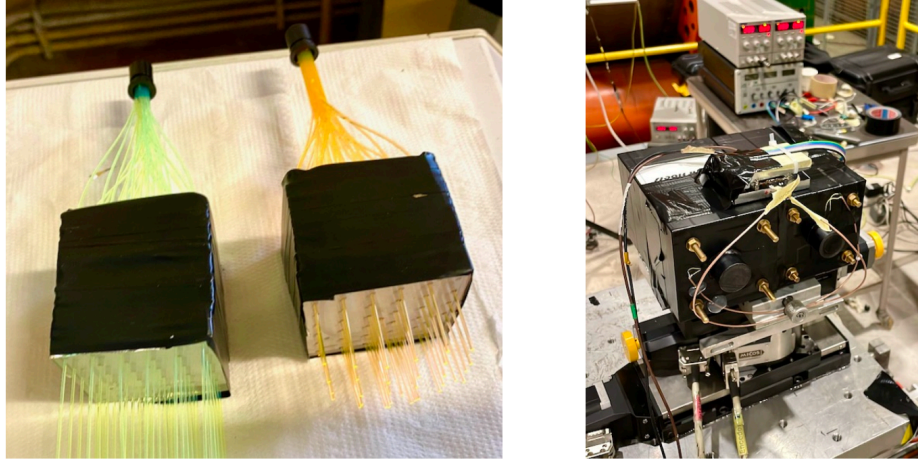

Fig. 5: Small shashlyk prototypes tested in fall 2022, during construction (left) and on the H2 beam line for testing (right).

Although current information suggests that optimized formulations of conventional polystyrene scintillator are sufficiently luminous, fast, and radiation resistant, in synergy with the AIDAinnova project NanoCal, we are evaluating the advantages that can be obtained with less conventional choices for the light emitter. In 2022, we participated in a recent head-to-head experimental comparison of small shashlyk prototypes made from conventional scintillator, specifically, the extrusion-moulded polystyrene scintillator formulated at IHEP Protvino for KOPIO, with 1.5% PTP and 0.04% POPOP, and a nanocomposite scintillator consisting of 0.2% cesium lead bromide ($CsPbBr_3$) nanocrystals in PMMA [17]. The latter, which emits in the green at 520 nm, is expected to be a very fast and bright alternative to conventional scintillators; its comparatively long wavelength emission and use of PMMA as a matrix material is expected to confer good radiation hardness. Identical prototypes consisting of 12 layers of 0.6-mm lead and 3-mm scintillator were constructed out of components from the PANDA/KOPIO calorimeter (**Fig. 5**); the nanocomposites fr this project were synthesized by collaborators at the University of Milano Bicocca and Glass To Power SpA, Rovereto. For the conventional prototype, the original scintillating tiles were used with Kuraray Y-11(200) green-emitting WLS fibre. The nanocomposite prototype used Kuraray O-2(100) orange-emitting WLS fibre. Each was read out with a single Hamamatsu 13360-6050 SiPM (6×6 mm^2, 50 μm pixel size) and fast amplifier with a gain of 4. In these tests, the conventional prototype showed significantly more light output than the nanocomposite prototype. To determine whether the luminosity and attenuation length of the orange fibres plays a significant role, a series of tests were carried out in June of 2023 to explore different fibre-scintillator pairings (including the use of custom-produced fibres).
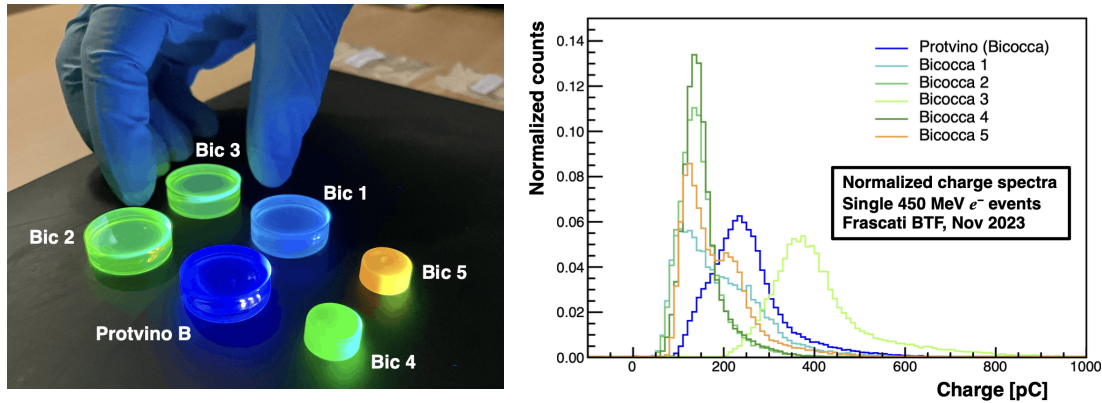
Fig. 6: Left: Nanocomposite scintillator samples tested at CERN and LNF in fall 2023. Right: Preliminary measurements of light yields from beam test at the BTF in fall 2023.

However, the results of these tests indicated no significant improvements in the light yields. During the remainder of 2023, therefore, the emphasis of the project was on the identification of a more suitable composition for the nanocomposite scintillator.

One idea, which was tested during the June 2023 beam test, was to incorporate a wavelength shifting dye into the nanocomposite. Specifically, about half of the bromine atoms in the $CsPbBr_3$ nanocrystals were substituted with chlorine atoms, shifting the primary emission from green to blue, and coumarin-6 was added to shift the emission back to the green, increasing the Stokes shift of the composite. Because the surface passivation of the nanocrystals was partially destroyed during the substitution reaction, leading to aggregation and giving rise to a milky appearance and poor transparency of the composite, this test was inconclusive; with ab initio synthesis of the mixed-halide nanocrystals, the technique may yet prove useful for nanocomposite optimization.

Meanwhile, we have focused on the development of nanocomposites with an aromatic matrix material, to facilitate energy transfer from the matrix to the nanocrystals. The samples shown in **Fig. 6,** left, were prepared at the University of Milano Bicocca for testing at the CERN PS and Frascati BTF in fall 2023. They all use PVT as the matrix material. The sample "Protvino B" uses the same dyes as the original Protvino scintillator, and samples Bicocca 1-3 are conventional molecular scintillators as control samples. Bicocca 2 and 3 use coumarin-6 as a WLS material, in addition to other dyes. Bicocca 4 and 5 are nanocomposites based on ytterbium-passivated $CsPbBr_3$ with the addition of 1.5% PTP; Bicocca 5 uses the perylene dye used in the WLS fibers to shift the emission to orange. Preliminary light yield measurements from the BTF are shown in **Fig. 6,** right. The two nanocomposite samples, Bicocca 4 and 5, have approximately half the light yield of the "Protvino B" sample and about the same light yield as the conventional scintillator samples Bicocca 1 and 2. Thus, the Bicocca 4 and 5 samples are the first nanocomposites that we have studied for which a significant light output is obtained. These results indicate that the PVT-based nanocomposites are a promising alternative, and five new samples (in addition to four new control samples without

nanocrystals) have been prepared for testing in 2024. Once a promising candidate has been identified, we are ready to proceed with the construction of new prototypes.

As a side note, **Fig. 6** shows that the Bicocca 3 sample, a conventional scintillator based on primary dyes of PTP and benzothiophene with coumarin-6 as a wavelength shifter, gives significantly more light than the "Protvino B" control sample, indicating that this could be a promising candidate as a bright, green-emitting scintillator whose comparatively long emission wavelength might be expected to confer additional radiation resistance.

HIKE Small-Angle Calorimeter and CRILIN

An ideal solution for a small-angle calorimeter for HIKE, capable of sustaining the expected rates and relatively transparent to beam neutrons during the K_L phases, is a highly granular, longitudinally segmented, fast crystal calorimeter, as conceptually illustrated in **Fig. 7.**
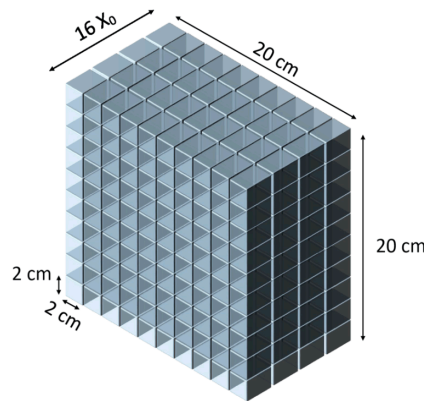

Fig. 7: Dimensional sketch of a SAC for KLEVER based on dense, high-Z crystals with both transverse and longitudinal segmentation.

CRILIN, an electromagnetic calorimeter under development for the International Muon Collider Collaboration [18], is an independently proposed, highly granular, longitudinally segmented, fast crystal calorimeter with SiPM readout and performance requirements similar to those for the HIKE SAC. Much development work for the HIKE SAC is being carried out in collaboration with the LNF CRILIN group (RD_MUCOL; see separate report), with particular emphasis on the SiPMs, front-end electronics, and signal readout, as well as on solutions for detector mechanics and SiPM cooling. The first test beam measurements with individual PbF$_2$ and PWO crystals were performed in summer 2021 at the Frascati BTF and the SPS North Area, followed by additional tests in fall 2022, in which some of the first commercially available samples of a new, ultra-fast formulation of PWO (PWO-UF) [15] were also tested. These tests were focused on understanding the best possible time resolution that can be obtained, studying the systematics of light collection in the small crystals, and validating the CRILIN choices of SiPMs and the design of the readout amplifier. In

autumn 2022, single $10 \times 10 \times 40$ mm^3 crystals of PbF$_2$ ($4.3X_0$) and PWO-UF ($4.5X_0$) were exposed to high-energy (60–120 GeV) electron beams at the SPS H2 beamline. Each crystal was viewed by a matrix of four Hamamatsu 14160-4010 SiPMs (4×4 mm^2, 10 μm pixel size), which were read out in pairs, providing independent readout channels for the left and right sides of the crystal. The SiPM was chosen to represent a plausible choice in the current state of the art for high-speed response, short pulse width, and good radiation resistance. The signals from the SiPMs were amplified with the CRILIN electronics and digitized at 5 GS/s. The data collected were analyzed and published in early 2023 [20], with the following conclusions:

- The time resolution obtainable from the combination of either crystal, PbF$_2$ or PWO-UF, with the chosen SiPM and CRILIN electronics is excellent, with the final time resolution expected to be significantly better than required for the KLEVER SAC. The time resolution is better when the detector is turned so that the SiPMs are on the upstream ends of the crystals, viewing downstream, as illustrated by the black curves in **Fig. 8,** from which it is seen that, for energy deposits of greater than 5 GeV, a time resolution of 15 ps or better is obtained with PbF2, and 20 ps or better with PWO-UF.
- The light yield for PWO-UF is approximately twice that for PbF$_2$; the time resolution for PbF$_2$ is slightly better.
- For either crystal, the light produced is highly localized on the rear face of the short crystal, requiring some care with the segmented readout.
- The CRILIN electronics performed very well; KLEVER should evaluate the possibility of faster shaping to obtain better double pulse discrimination.
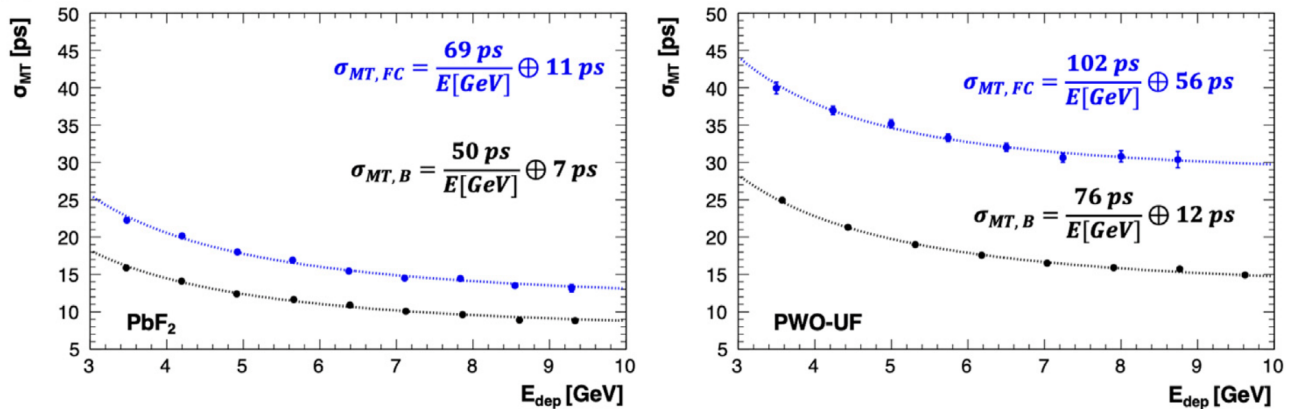

Fig. 8: Mean time resolution for two crystals, from CRILIN test beam, fall 2022: PbF$_2$, left, and PWO-UF, right. Blue and black curves are for configuration in which SiPM is mounted downstream facing upstream and vice versa, respectively. Reproduced from [20].

The next step of CRILIN development was then to test a two-layer, 3×3 crystal array developed in 2021-2022 [18]. The light is read out in the same manner as for the single crystals tested in 2022, with two channels per crystal, for a total of 36 channels. Modular electronics for power distribution, SiPM signal processing, and control were also developed.

After a short test in the CERN PS T9 area in June 2023, the two-layer, 3 × 3 crystal CRILIN prototype was tested extensively with 450 MeV electrons at the Frascati BTF in June 2023, with 20-120 GeV electrons and 40 GeV mips at the SPS H2 beamline in August 2023, and again in October 2023 in the T9 area with 4 GeV electrons. The purpose of these tests was to validate the segmentation scheme, measure the time resolution with reconstructed clusters, study the effects of design optimizations such as the choice of crystal surface treatments and wrapping materials, and evaluate the performance of the engineering solutions adopted. In the October 2023 test, the response of the prototype was also studied as a function of the alignment of the beam with axes of the central PWO-UF crystal on which the beam was incident. **Fig. 9** shows the prototype during alignment on the T9 beamline during the October 2023 test.
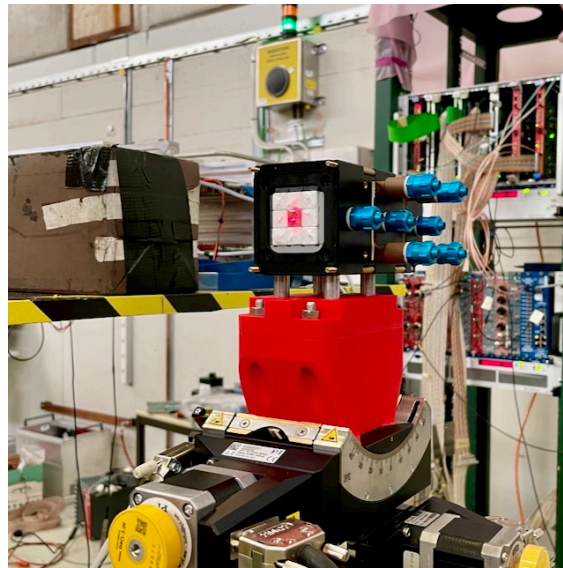

Fig. 9: CRILIN prototype during alignment on T9 beamline during the October 2023 test at the CERN PS.

Although the data collected during the summer and fall 2023 test beams are still under analysis, some preliminary findings are already apparent. Among the various techniques for crystal surface preparation and wrapping, the best time resolution was obtained with ground crystal surfaces and Teflon wrapping as a diffuse reflector. With this wrapping scheme, the single-crystal time resolution for PbF_2 as measured from Δt was seen to improve from 12 ps to 9 ps. A first attempt at the time resolution for cluster reconstruction was limited by two aspects of the readout system. The time resolution as measured from Δt between layers has been estimated preliminarily to be about 40 ps, dominated by the synchronization jitter between DRS4 chips in the CAEN V1742 digitizer boards used. The absolute time resolution measured with respect to a fast scintillator used as a time reference is dominated receives and additional contribution from the reference detector. Work is in progress to minimize both contributions. The distributions of the energy deposited in each crystal and in the entire assembly were measured and compared to results from the simulation described in [20], with excellent

agreement, which was facilitated by the use of SiPMs from the same production lot with good gain uniformity.

PUBLISHED PAPERS

1) Search for dark photon decays to $\mu^+\mu^-$ at NA62
E. Cortina Gil et al., NA62 Collaboration, JHEP 09 (2023) page 035
doi.org/10.1007/JHEP09(2023)035, arXiv2303.08666 [hep-ex].

2) Improved calorimetric particle identification in NA62 using machine learning techniques
E. Cortina Gil et al., NA62 Collaboration, JHEP 11 (2023) 138,
doi.org/10.1007/JHEP11(2023)138, arXiv:2304.10580 [hep-ex].

3) A study of the $K^+ \rightarrow \pi^0 e\nu\gamma$ decay
E. Cortina Gil et al., NA62 Collaboration, JHEP 09 (2023) 040,
doi.org/10.1007/JHEP09(2023)040, arXiv:2304.12271 [hep-ex].

4) Search for K^+ decays into the $\pi^+ e^+ e^- e^+ e^-$ final state
E. Cortina Gil et al., NA62 Collaboration, Phys. Lett. B 846 (2023) 138193,
doi.org/10.1016/j.physletb.2023.138193, arXiv:2307.04579 [hep-ex].

5) Measurement of the $K^+ \rightarrow \pi^+ \gamma\gamma$ decay
E. Cortina Gil et al., NA62 Collaboration, Phys. Lett. B 850 (2024) 138513,
doi.org/10.1016/j.physletb.2024.138513, arXiv:2311.01837 [hep-ex].

6) Search for leptonic decays of the dark photon at NA62
E. Cortina Gil et al., NA62 Collaboration, accepted for publication in Phys. Rev. Lett., arXiv.2312.12055 [hep-ex].

7) Development of a new CEDAR for kaon identification at the NA62 experiment at CERN
A. Bethani et al., NA62 Collaboration, accepted for publication in JINST, arXiv.2312.17188 [hep-ex].

REFERENCES

8) E. Cortina Gil et al. (NA62 Collaboration), "The Beam and detector of the NA62 experiment at CERN", JINST 12 (2017) P05025
doi.org/10.1088/1748-0221/12/05/P05025

9) E. Cortina Gil et al. (NA62 Collaboration), "First search for the $K^+ \to \pi^+ \nu \bar{\nu}$ decay using the decay-in-flight technique", Phys. Lett. B 791 (2019) 156
doi.org/10.1016/j.physletb.2019.01.067

10) E. Cortina Gil et al. (NA62 Collaboration), "An investigation of the very rare $K^+ \to \pi^+ \nu \bar{\nu}$ decay", J. High Energ. Phys. 2011 (2020) 042
doi.org/10.1007/JHEP11(2020)042

11) Measurement of the very rare $K^+ \to \pi^+ \nu \bar{\nu}$ decay
E. Cortina Gil et al. (NA62 collaboration), J. High Energ. Phys. 2106 (2021) 093
doi.org/10.1007/JHEP06(2021)093

12) F. Ambrosino et al. (KLEVER Project), "KLEVER: An experiment to measure $BR(K_L \to \pi^0 \nu \bar{\nu})$ at the CERN SPS", prepared for the 2020 update of the European Strategy for Particle Physics, arXiv:1901.03099 [hep-ex]

13) E. Cortina Gil et al. (HIKE Collaboration), "HIKE, High Intensity Kaon Experiments at the CERN SPS: Letter of Intent", CERN-SPSC-2022-031, SPSC-I-257, November 2022, arXiv:2211.16586 [hep-ex]

14) M. U. Ashraf et al. (NA62 collaboration), "High Intensity Kaon Experiments (HIKE) at the CERN SPS: Proposal for Phases 1 and 2", CERN Proposal CERN-SPSC-2023-031, SPSC-P-368, October 2023, arXiv:2311.08231 [hep-ex]

15) V. Fanti et al., "The beam and detector for the NA48 neutral kaon CP violation experiment at CERN", Nucl. Instrum. Meth. A 574 (2007) 433
doi.org/10.1016/j.nima. 2007.01.178

16) G. S. Atoian et al., "An Improved Shashlyk Calorimeter", Nucl. Instrum. Meth. A584 (2008) 291
doi.org/10.1016/j.nima.2007.10.022

17) A. Erroi et al., "Ultrafast and Radiation-Hard Lead Halide Perovskite Nanocomposite Scintillators", ACS Energy Lett. 8 (2023) 3883
https://doi.org/10.1021/acsenergylett.3c01396

18) S. Ceravolo et al., "Crilin: A CRystal calorImeter with Longitudinal InformatioN for a future Muon Collider", J. Instrum. 17.09 (2022) P09033
doi.org/10.1088/1748-0221/17/ 09/P09033

19) M. Korzhik et al., "Ultrafast PWO scintillator for future high energy physics instrumentation", Nucl. Instrum. Meth. A 1034 (2022) 166781
doi.org/10.1016/j.nima.2022.166781

20) C. Cantone et al., "Beam test, simulation, and performance evaluation of PbF2 and PWO-UF crystals with SiPM readout for a semi-homogeneous calorimeter prototype with longitudinal segmentation", Front. Phys. 11 (2023) 1223183 doi.org/10.3389/fphy.2023.1223183

21) Moriond QCD International Workshop, https://moriond.in2p3.fr/2024/QCD/Program.html

CONFERENCE TALKS

S. Martellotti:
- Latest results and precision measurements from the NA62 experiment, Alpine Particle Physics Symposium (ALPS 2023), Obergurgl, Austria, 27 March 2023
- Status and prospects of rare decays at NA62/HIKE, Workshop Italiano sulla Fisica ad Alta Intensità (WIFAI 2023), Rome, Italy, 09 November 2023

M. Moulson:
- Kaon decays and the Cabibbo Angle Anomaly, 12th International Workshop on the CKM Unitarity Triangle (CKM 2023), Santiago de Compostela, Spain, 20 September 2023

M. Soldani:
- Physics Beyond the Standard Model with the NA62 experiment at CERN First African Conference on High-Energy Physics (ACHEP 2023), Rabat, Morocco, 27 October 2023

G. Tinti:
- Physics beyond the Standard Model with NA62, New Frontiers in Lepton Flavor, Pisa, Italy, 15 May 2023